Experimental determination of the topological phase diagram by soft X-ray angle-resolved photoemission spectroscopy

The discovery of topological insulators represents significant progress in topological band theory [1]. They are characterized by a nontrivial Z_2 topological invariant (ν_0: $\nu_1\nu_2\nu_3$); each of these four invariants takes a value of either 0 or 1, indicating 16 phases with three general classes according to Ref. 1. This nontrivial Z_2 invariant can be realized only if the conduction and valence bands are inverted by spin-orbit coupling (SOC). In the three-dimensional case, the band inversion gives rise to topological surface states (TSSs) inside the energy gap. Owing to the bulk-edge correspondence, investigations of the in-gap TSS in principle can reveal the band topology of the bulk states. In fact, surface-sensitive angle-resolved photoemission spectroscopy (ARPES) with vacuum ultraviolet (VUV) light has achieved great success in confirming the Dirac-cone-like TSS in a number of chalcogenides and obtained excellent agreement with the predicted nontrivial Z_2 topology [1].

However, searches of the topological phase are still challenging in low-carrier semimetals such as rare-earth monopnictides LnX (Ln: La or Ce; X: P, As, Sb, or Bi). The main difficulty comes from two issues. One is that a band calculation can lead to controversial conclusions about their band topology [2], since the magnitude of band gaps can often be misestimated in such low-carrier systems, and thus the experimental determination is crucial. Secondly, despite this, the experimental confirmations have so far been limited to the observation of the surface dispersions predicted by calculations [3,4]. In this study, we present an alternative approach to determine the band topology by means of bulk-sensitive soft X-ray ARPES (SX-ARPES) [5]. For this demonstration, we adopt a series of materials of CeX. By the paradigmatic investigation of the electronic structures from CeP to CeBi as a function of their SOC, we draw the topological phase diagram and unambiguously reveal the topological phase transition from a trivial to a nontrivial regime induced by the band inversion.

Single crystalline CeX's were grown by the Bridgman method. Bulk-sensitive SX-ARPES measurements were performed at SPring-8 **BL25SU**. The total experimental energy resolution was set to about 70–90 meV for photon energies ($h\nu$) of 500–760 eV. All samples were cleaved at a pressure of 5×10^{-8} Pa at approximately 60 K, exposing shiny surfaces corresponding to the (001) plane of the NaCl crystal structure.

We start with comparing the bulk electronic structures of the CeX's. By tuning $h\nu$ in the SX range, we observe their bulk band dispersions selectively cut along the high-symmetry X-Γ-X line (Fig. 1). By systematically examining the electronic structures, we find the SOC effect and its evolution. We find three important consequences of the SOC. Firstly, valence bands at Γ point originating from pnictogen *p* orbitals split into the $p_{1/2}$ and $p_{3/2}$ states. The magnitude of the splitting varies substantially across the series of compounds. Secondly, the SOC also induces valence band splitting at the X point. The large SOC pushes the X1 (X2) band up (down) in energy [red (green) arrows in Fig. 1]. The splitting becomes significant with increasing SOC. Thirdly, for CeSb and CeBi, the

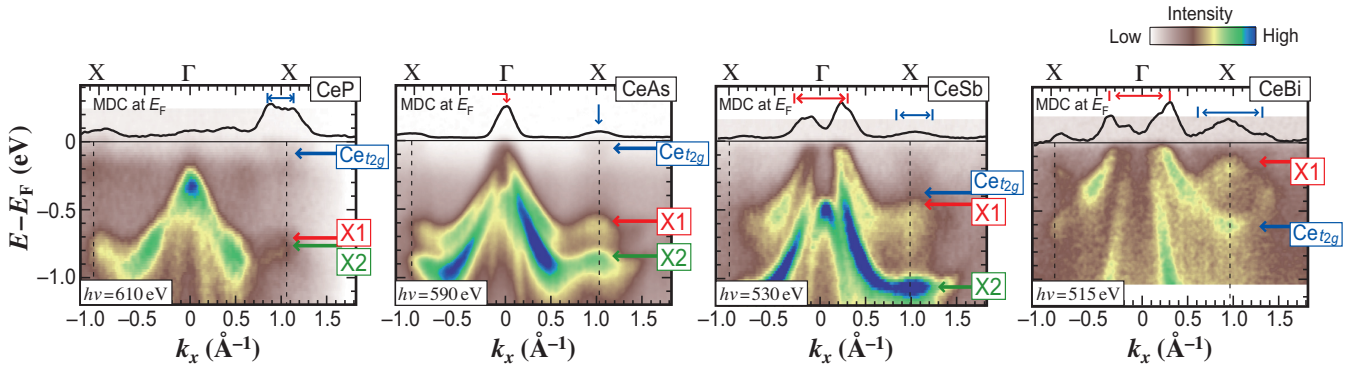

Fig. 1. SX-ARPES band maps and (inset) their momentum distribution curves (MDCs) for CeX's obtained at $h\nu$ of (CeP) 610 eV, (CeAs) 590 eV, (CeSb) 530 eV, and (CeBi) 515 eV, cut along the high symmetry X-Γ-X line in the 3D Brillouin zone. The hole X1 (Ce_{t2g} electron) bands are shown by red (blue) arrows.

higher-lying $p_{3/2}$ bands at the Γ point are pushed above E_F due to the large SOC, and hole pockets appear [red arrows in inset].

The third effect triggers a dynamical change in the Ce_{t2g} electron band. The SOC evolution of the hole pockets should increase the size of the electron pocket at the X point to compensate their carriers, since the CeX series materials have a similar low carrier density. This carrier compensation is necessary in the semimetallic structure of CeX's. This electron band evolution is captured by blue arrows in Fig. 1. For CeAs, both the hole and electron pockets are quite small. With the increasing size of the hole pocket at the Γ point from CeAs to CeBi, the electron band bottom appears to decrease energy. This eventually leads to the band inversion in CeBi.

On the basis of the SX-ARPES results, one can now draw the topological phase diagram of CeX's (Fig. 2). The topological phase transition is elucidated by SOC in collaboration with the carrier compensation of the semimetallic structures. CeSb is trivial but close to a phase transition state, whereas CeBi is classified into a nontrivial phase owing to the band inversion. The band inversion process visualized by SX-ARPES is the most fundamental feature of the topological matter; therefore, the presented nontrivial topology of CeBi is identified without surface information.

In summary, we performed bulk-sensitive SX-ARPES on CeX series materials and determined the topological phase diagram. Our experiment unambiguously demonstrated the topological transition from a trivial to a nontrivial phase across the border between CeSb and CeBi in the presented phase diagram. Moreover, the mechanism is explained by SOC in concert with the carrier-compensated semimetallic band structures. This work demonstrates a new capability of SX-ARPES to clarify the band topology, which can be widely applied for solid states as a complementary tool to surface-sensitive ARPES.

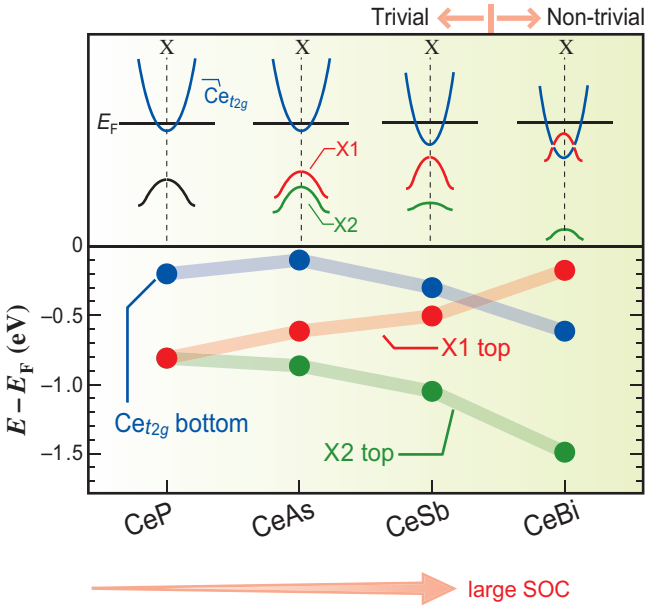

Fig. 2. Experimentally determined topological phase diagram with the energy positions of (blue) Ce_{t2g}, (red) X1, and (green) X2 bands. (Inset) Schematics of the band structures around X point.

Kenta Kuroda* and Takeshi Kondo

The Institute for Solid State Physics,
The University of Tokyo

*Email: kuroken224@issp.u-tokyo.ac.jp

References

[1] M.Z. Hasan and C.L. Kane: Rev. Mod. Phys. **82** (2010) 3045.
[2] P.-J. Guo *et al.*: Phys. Rev. B **93** (2016) 235142.
[3] X.H. Niu *et al.*: Phys. Rev. B **94** (2016) 165163.
[4] L. Meng *et al.*: Phys. Rev. Lett. **117** (2016) 127204.
[5] *K. Kuroda, M. Ochi, H.S. Suzuki, M. Hirayama, M. Nakayama, R. Noguchi, C. Bareille, S. Akebi, S. Kunisada, T. Muro, M.D. Watson, H. Kitazawa, Y. Haga, T.K. Kim, M. Hoesch, S. Shin, R. Arita and T. Kondo: Phys. Rev. Lett.* ***120*** *(2018) 086402.*